J. W. (1988) *J. Biomol. Struct. Dyn. 5*, 1059.
Letovsky, J., & Dynan, M. S. (1989) *Nucleic Acids Res. 17*, 2639–2653.
Lown, J. W., Sondhi, S. W., Ong, C.-W., Skorobogaty, A., Kishikawa, H., & Dabrowiak, J. C. (1986) *Biochemistry 25*, 5111–5117.
Marky, L. A., & Breslauer, K. J. (1987) *Proc. Natl. Acad. Sci. U.S.A. 84*, 4359–4363.
McGhee, J. D., & von Hippel, P. H. (1974) *J. Mol. Biol. 86*, 469–489.
Rehfuss, R., Goodisman, J., & Dabrowiak, J. C. (1990) *Biochemistry 29*, 777–781.
Scamrov, A. V., & Beabealashvilli, R. S. (1983) *FEBS Lett. 164*, 97–99.
Schmitz, A., & Galas, D. J. (1979) *Nucleic Acids Res. 6*, 111–137.
Senear, D. F., Brenowitz, M., Shea, M. A., & Ackers, G. K. (1986) *Biochemistry 25*, 7344–7354.
Van Dyke, M. W., Hertzberg, R. P., & Dervan, P. B. (1982) *Proc. Natl. Acad. Sci. U.S.A. 79*, 5470–5474.
Ward, B., Rehfuss, R., & Dabrowiak, J. C. (1987) *J. Biomol. Struct. Dyn. 4*, 685–695.
Ward, B., Rehfuss, R., Goodisman, J., & Dabrowiak, J. C. (1988a) *Biochemistry 27*, 1198–1205.
Ward, B., Rehfuss, R., Goodisman, J., & Dabrowiak, J. C. (1988b) *Nucleic Acids Res. 16*, 1359–1369.
Zimmer, C., & Wahnert, V. (1986) *Prog. Biophys. Mol. Biol. 47*, 31–112.

Preferential Binding of Daunomycin to 5′$\frac{A}{T}$CG and 5′$\frac{A}{T}$GC Sequences Revealed by Footprinting Titration Experiments†

Jonathan B. Chaires* and Julio E. Herrera
Department of Biochemistry, University of Mississippi Medical Center, Jackson, Mississippi 39216-4505
Michael J. Waring
Department of Pharmacology, Medical School, University of Cambridge, Cambridge CB2 2QD, United Kingdom
Received November 30, 1989; Revised Manuscript Received February 16, 1990

ABSTRACT: Results from a high-resolution deoxyribonuclease I (DNase I) footprinting titration procedure are described that identify preferred daunomycin binding sites within the 160 bp *tyr T* DNA fragment. We have obtained single-bond resolution at 65 of the 160 potential binding sites within the *tyr T* fragment and have examined the effect of 0–3.0 μM total daunomycin concentration on the susceptibility of these sites toward digestion by DNase I. Four types of behavior are observed: (i) protection from DNase I cleavage; (ii) protection, but only after reaching a critical total daunomycin concentration; (iii) enhanced cleavage; (iv) no effect of added drug. Ten sites were identified as the most strongly protected on the basis of the magnitude of the reduction of their digestion product band areas in the presence of daunomycin. These were identified as the preferred daunomycin binding sites. Seven of these 10 sites are found at the end of the triplet sequences 5′$\frac{A}{T}$GC and 5′$\frac{A}{T}$CG, where the notation $\frac{A}{T}$ indicates that either A or T may occupy the position. The remaining three strongly protected sites are found at the ends of the triplet sequence 5′$\frac{A}{T}$C$\frac{A}{T}$. Of the preferred daunomycin binding sites we identify in this study, the sequence 5′$\frac{A}{T}$CG is consistent with the specificity predicted by the theoretical studies of Chen et al. [Chen, K.-X., Gresh, N., & Pullman, B. (1985) *J. Biomol. Struct. Dyn. 3*, 445–466] and is the very sequence to which daunomycin is observed to be bound in two recent X-ray crystallographic studies. Solution studies, theoretical studies, and crystallographic studies have thus converged to provide a consistent and coherent picture of the sequence preference of this important anticancer antibiotic.

The cellular target of many clinically useful anticancer compounds is thought to be DNA (Gale et al., 1981; Chagas & Pullman, 1987). A necessary step toward the rational design of new anticancer compounds with enhanced potency and selectivity is to characterize the DNA binding specificity of these existing compounds of proven clinical utility and to elucidate the molecular mechanisms that govern their sequence-selective binding to DNA. It is hoped that this activity will produce, ultimately, a set of rules to guide the rational design of a new generation of anticancer compounds targeted to specific DNA sites.

With this larger goal in mind, our laboratory has studied the interaction of daunomycin with DNA by a variety of physical and biochemical methods (Britt et al., 1986; Chaires, 1983a,b, 1985a,b; Chaires et al., 1982a,b, 1983, 1985, 1987; Herrera & Chaires, 1989; Fritzsche et al., 1982, 1987). Daunomycin is the prototype anthracycline antibiotic, a class of compounds that has well-documented utility in cancer chemotherapy (Arcamone, 1981; Crooke & Reich, 1980; Remers, 1984). Daunomycin binds to DNA by the process of intercalation, and the fundamental aspects of the physical chemistry of its binding to DNA have been well characterized [for reviews, see Fritzsche and Berg (1987) and Chaires

†Supported by U.S. Public Health Service Grant CA35635, awarded by the National Cancer Institute, Department of Health and Human Services, National Science Foundation Grant INT-8521004 (J.B.C.), and grants from the Cancer Research Campaign (M.J.W.).

0006-2960/90/0429-6145$02.50/0

(1990a)]. Whether or not daunomycin binds preferentially to particular DNA sequences, however, has been a vexing question, and the published literature is both confusing and contradictory [reviewed in Neidle and Sanderson (1983), Saenger (1984), and Chaires (1983b)]. An important indication of the sequence specificity of daunomycin binding to DNA was provided by the theoretical studies of the Pullman group (Chen et al., 1985). These studies suggested that a triplet sequence was recognized as a preferred site by daunomycin, with the sequences 5′ACG and 5′TCG being the most energetically favored sites of those studied. DNase I footprinting studies (Chaires et al., 1987) established that daunomycin does indeed recognize preferred sites along the DNA lattice and that these sites all contained triplet sequences of the type predicted by the theoretical studies. However, another DNase I footprinting study identified the dinucleotide sequence 5′CA as the preferred daunomycin binding site (Skorobogaty et al., 1988a,b). The origin of this apparent discrepancy is not clear; it may arise from differences either in interpretation or in the primary data itself. In both studies, the sites protected from DNase I digestion by bound daunomycin were broad, and data were obtained over a limited range of drug concentrations. Higher resolution footprinting data are needed to more clearly define preferred daunomycin binding sites.

We report here results obtained by a high-resolution DNase I footprinting titration method that provide a more refined view of preferred daunomycin binding sequences. These footprinting titration experiments afford single nucleotide resolution of preferred drug binding sites and can, in principle, be used to estimate microscopic binding constants for ligand binding to individual sites along the DNA lattice (Brenowitz et al., 1986; Dabrowiak & Goodisman, 1989; Tullius, 1989; Ward et al., 1987, 1988a,b). While we have not yet reached the latter level of sophistication, our data enable us to identify the triplet sequences 5′$\overset{A}{T}$CG and 5′$\overset{A}{T}$GC as the most preferred daunomycin binding sites. These new results both extend and confirm our results from previous footprinting studies and are in excellent agreement with theoretical predictions (Chen et al., 1985). The combined results from our studies in solution, theoretical studies (Chen et al., 1985), and recent high-resolution crystallographic studies of daunomycin–hexanucleotide complexes (Wang et al., 1987; Moore et al., 1989) make the daunomycin–DNA interaction one of the best characterized intercalation reactions at the molecular level. The possible molecular determinants of daunomycin's sequence preference may now be described in some detail.

Materials and Methods

Materials. Daunomycin was obtained from Sigma Chemical Co. (St. Louis, MO) and was used without further purification. A 1 mM stock daunomycin solution (in 10 mM Tris buffer, 10 mM NaCl, pH 7.5) was prepared and stored in the dark at 4 °C. An extinction coefficient of 11 500 M^{-1} cm^{-1} was used to determine daunomycin concentrations from absorbance measurements at 480 nm. Deoxyribonuclease I (DNase I) was purchased from Sigma Chemical Co. (St. Louis, MO) and was stored at −20 °C at a concentration of 7200 units mL^{-1} in a solution containing 150 mM NaCl and 1 mM $MgCl_2$. Aliquots of this enzyme stock solution were diluted to working concentrations immediately before use, using as a dilution buffer a solution containing 20 mM NaCl, 2 mM $MgCl_2$, and 2 mM $MnCl_2$.

DNA Fragment for Footprinting Experiments. A 160 bp duplex DNA fragment containing the tyrosine tRNA promoter (the "*try T* fragment") was isolated and labeled with ^{32}P as previously described (Drew & Travers, 1984; Low et al., 1984a,b).

DNase I Footprinting Titration Experiments. Footprinting reactions were done in a total volume of 12 μL at a temperature of 4 °C. Samples (2 μL) of the labeled *try T* fragment were incubated with 8 μL of buffer solution (10 mM Tris, 10 mM NaCl, pH 7.5) containing the desired daunomycin concentration. These incubations were at 4 °C for a duration of at least 2 h to ensure equilibration of the binding reaction. The digestion reaction was initiated by the addition of 2 μL of a DNase I stock solution whose concentration was adjusted to yield a final enzyme concentration of 0.01 unit mL^{-1} in the reaction mixture. After 5 min, the digestion was stopped by the addition of 5 μL of an 80% formamide solution containing 10 mM EDTA and 0.1% bromophenol blue. Samples were then heated at 100 °C for 2 min prior to electrophoresis.

The products of the DNase I digestion of the *try T* fragment were analyzed on 0.3-mm 8% (w/v) polyacrylamide gels containing 7 M urea and Tris–borate–EDTA buffer, pH 8.3. Electrophoresis was at 1500 V for 2 h. Following electrophoresis, gels were soaked in 10% acetic acid for 10 min, transferred to Whatman 3MM paper, and dried under vacuum at 70 °C. Product bands were visualized by autoradiography at −70 °C on an intensifying screen or at room temperature without the intensifying screen. The latter procedure provided autoradiograms with sharper bands and finer resolution and was used for data to be subjected to quantitative densitometric analysis.

Densitometry. Autoradiograms were scanned by using a BioRad 620 video densitometer interfaced to an IBM AT computer for instrument control, data acquisition, and data reduction. The lane on the autoradiogram to be scanned and digitized was manually centered on an illuminated slit 20 cm long and 2 mm wide. Transmitted light from the slit is focused onto a 1728 element linear diode array, which digitizes the entire image of the autoradiogram lane after collecting 64 sample images each of 100-ms duration for signal averaging. The one-dimensional scan of the 20-cm region of the autoradiogram consists of 3320 data points acquired in 6.4 s. The digitized scan is displayed in real time for subsequent analysis and correction. The stated resolution of the instrument is 330 μM. A typical band on the autoradiogram was 0.5–1.0 mm in the vertical dimension and 6 mm in the horizontal dimension.

Data Reduction. The digitized scan was corrected in two steps. First, a blank region of the autoradiogram was scanned and subtracted from all subsequent scans as a background correction. Second, a base line was established by connecting line segments to discrete minima within the one-dimensional scan. Figure S1 (supplementary material) shows sample scans obtained from the autoradiogram shown in Figure 1. Peaks were manually selected, and peak areas determined by integration using manually defined limits. Single-band resolution on the autoradiogram was obtained for positions 80–125 (according to the numbering scheme shown in Figure 6). Additional peaks outside this region were resolved if their intensity was sufficiently high. Each resolved band on the autoradiogram was assigned to a particular bond within the *try T* DNA sequence by comparison of its position relative to the products of a Maxam–Gilbert guanine-specific reaction analyzed on the same gel. Peak areas were stored on a disk as an ASCII file and subsequently transferred into a SuperCalc spread sheet for statistical and preliminary graphical analysis. The final data set obtained consisted of 65 band positions, for which data were obtained at seven total daunomycin concen-

trations. The error associated with the densitometry and data reduction procedure was determined by averaging 12 separate scans of each lane on the autoradiogram and calculating the mean and standard deviation. Over 5000 individual peak areas were thus determined in the analysis of our data. Figure S2 shows the percent error determined as a function of the mean peak area. It is not surprising that smaller peak areas are determined with less precision.

Linearity of Response. The response curve for the combined autoradiograph/densitometry procedure was determined by preparing serially diluted samples of the ^{32}P labeled *try T* DNA fragment and performing the gel electrophoresis, autoradiography, and densitometry as described above on the undigested fragment. DNA concentrations were defined relative to the total amount of DNA normally loaded per lane. Figure S3 (supplementary material) shows the response curve obtained. The response is essentially linear up to about 3.0 peak area units. In no case did the area of a product band used in our analysis exceed this value.

Normalization Procedure. Peak areas were corrected for slight differences in the total amount of labeled DNA loaded in each lane by normalizing to the integrated area of band 45 (a position whose area is unaffected by added daunomycin over the concentration range used in these studies) following the internal standard procedure of Brenowitz et al. (1986). The assertion that the area of band 45 is unaffected by added daunomycin is based on the inspection and analysis of over 38 separate footprinting titration experiments. Figure S4 (supplementary material) illustrates the average area of band 45 and the total product area over a daunomycin concentration range of 0–3.0 μM. The total product area declines smoothly with added daunomycin, an indication that the drug and enzyme compete for sites. In contrast, the area of band 45 is essentially constant (within experimental error) up to a daunomycin concentration of 1.5–2.0 μM added drug. Apparent peak areas A_i within a lane were normalized according to the relation

$$A_i^{corr} = A_i(A_{45}/A_{45}^0)$$

where A_{45} is the area of band 45 in the lane for which data is gathered and A_{45}^0 is the area of band 45 in the control lane with no added drug. The maximum correction applied by this procedure was 15–20%.

Results

An autoradiogram from a footprinting titration experiment for the interaction of daunomycin with the *try T* DNA fragment is shown in Figure 1. Inspection of the autoradiogram indicates a varied response at each position upon addition of antibiotic. Detailed analysis of primary data such as these requires quantitative densitometry, as described in detail in the Materials and Methods section. Such an analysis yields a collection of corrected peak areas as a function of daunomycin concentration for each resolved band in the autoradiogram. We have obtained single-band resolution for 65 positions in the autoradiogram shown in Figure 1, corresponding to information concerning the probability of DNase I cutting at 65 out of the 160 phosphodiester backbone bonds within a strand of the *tyr T* DNA fragment.

Four types of behavior have been observed at individual positions in response to the addition of DNase I. Selected examples of each type of behavior are shown in Figures 2–5 as footprinting titration plots in which the average peak area for a given position is plotted as a function of total added daunomycin concentration. The first class of sites, observed at 21 of the 65 resolved positions, are those that are protected

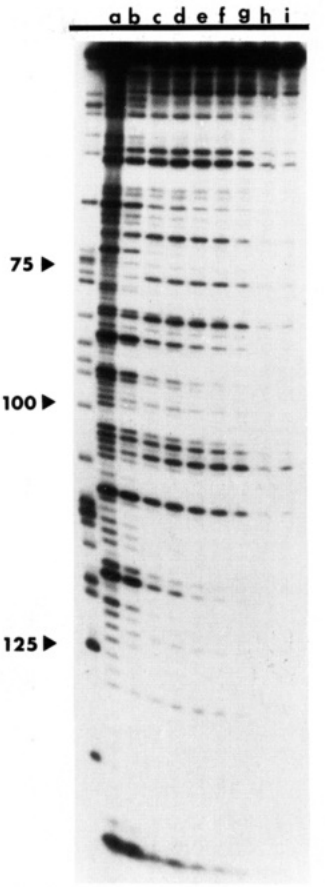

FIGURE 1: Autoradiogram of a footprinting titration experiment for the binding of daunomycin to the *try T* DNA fragment. The leftmost lane shows the products resulting from the Maxam–Gilbert dimethyl sulfate/piperidine reaction and indicates the location of guanine residues within the sequence. The remaining lanes show the products resulting from limited DNase I digestion of the *try T* DNA fragment in the presence of increasing concentration (expressed as micromolar) of added daunomycin, as follows: (a) 0; (b) 0.25; (c) 0.5; (d) 0.75; (e) 1.0; (f) 1.5; (g) 2.0; (h) 2.5; (i) 3.0. The numbers on the left indicate the bond position within the sequence presented in Figure 6.

from DNase I attack by added daunomycin, resulting in a smooth decrease in average peak area with added drug (Figure 2). A second class of protected site, observed at 19 positions, is shown in Figure 3. For these sites, protection occurs only after reaching a threshold total drug concentration. Initial additions of daunomycin appear to have little effect on the average peak area, but increased drug concentration results in a sharp decrease in peak area. Such behavior is subtle and was not detected in previous footprinting experiments, which used higher daunomycin concentrations, beyond the range in which the effect is observed. A third class of behavior, observed at four positions, is illustrated in Figure 4. Cleavage by DNase I is enhanced at these sites upon addition of daunomycin. The magnitude of the effect is dramatic. As shown in Figure 4, the average peak area may increase 4–5-fold over the control value. The fourth and final class of behavior, observed at 21 positions, is illustrated in Figure 5. The peak area at these positions is unaltered by addition of daunomycin, within the limits of experimental error. These sites are presumed to represent sites to which daunomycin will not bind.

Figure 6 summarizes the results of titration footprinting experiments on the *try T* DNA fragment. The quantity A_f/A_0, which is the ratio of the average peak area at the end point of the daunomycin titration to that in the absence of drug, is shown in Figure 6 for each resolved position within the se-

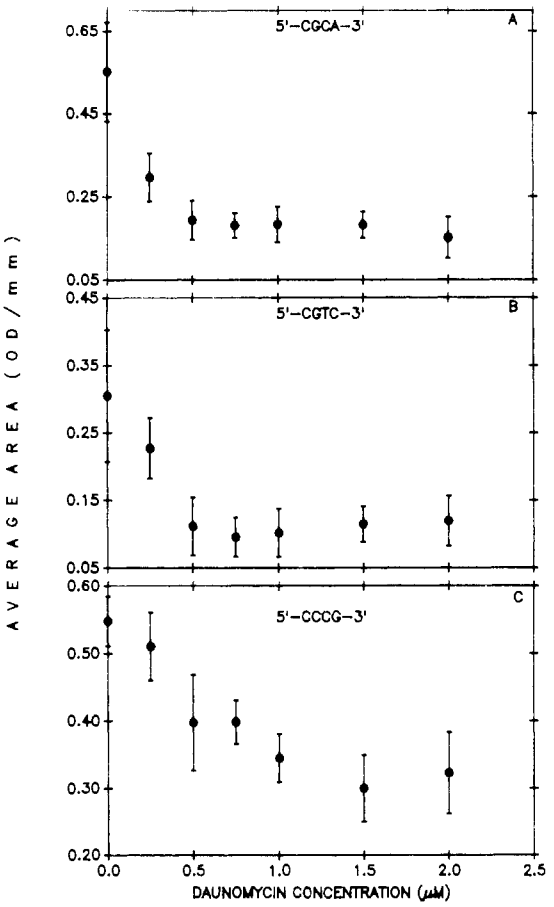

FIGURE 2: Selected examples of positions protected from DNase I attack by added daunomycin. The bond is between the central dinucleotide in the sequence shown at the top of each panel. Each pannel contains a point at 0 μM daunomycin concentration, which is partially obscured by the ordinate. These data are for the following positions within the sequence presented in Figure 6: (A) position 36; (B) position 79; (C) position 98.

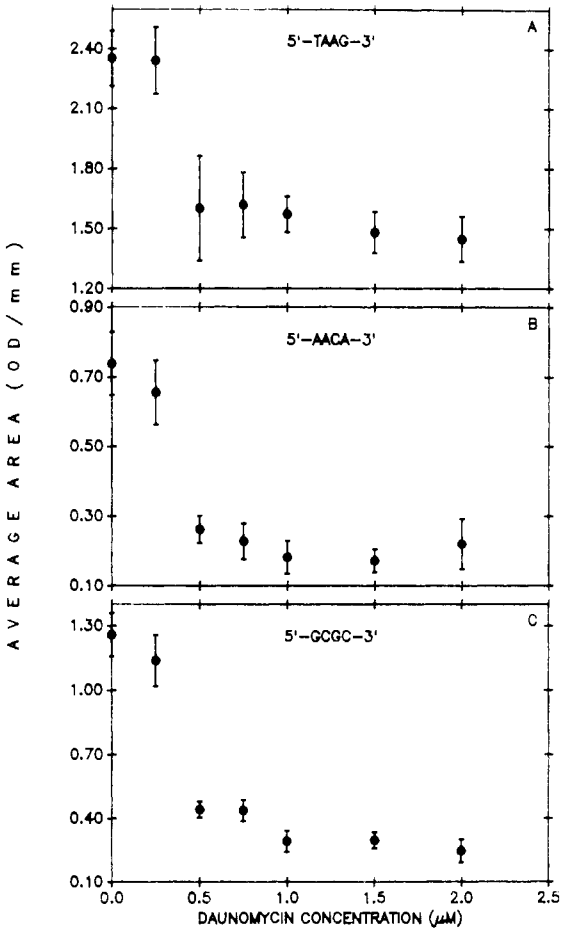

FIGURE 3: Selected examples of positions protected from DNase I attack by added daunomycin but only after a threshold concentration of drug is reached. These data are for the following positions within the sequence presented in Figure 6: (A) position 111; (B) position 62; (C) position 95.

quence. An A_f/A_0 value of 1.0 indicates no protection by daunomycin, while a value less than one indicates protection by daunomycin. A table that catalogs all of the protected sequences we have observed and a histogram showing the distribution of A_f/A_0 values is included in the supplementary material. An average value of $A_f/A_0 = 0.39 \pm 0.16$ was calculated for all protected sites. Site with A_f/A_0 values $\leq$ 0.27 (approximately one standard deviation lower than the mean) were identified as the most protected, and therefore the preferred, daunomycin binding sites.

Discussion

The results described here, obtained by using the footprinting titration method, are a substantial improvement over previous efforts that attempted to map preferred daunomycin DNA binding sites. The method is of higher resolution and allows the concentration dependency of daunomycin binding to individual sites to be examined. Our new results are fully consistent with our previous lower resolution DNase I footprinting experiments (Chaires et al., 1987) but afford a more exact specification of the preferred daunomycin binding sites along the DNA lattice. The footprinting titration method also reveals subtle behavior not previously observed in daunomycin footprinting experiments.

Strongly Protected Sites. The 10 sites most highly protected by daunomycin from digestion by DNase I are listed in Table I. These sites show the greatest reduction in integrated peak area in response to added daunomycin of all of the resolved

Table I: Strongly Protected Sites within the *try T* DNA Fragment[a]

position	sequence	A_f/A_0	$C_{1/2}$ (μM)
67	5'CTT TAC	0.12	0.25
70	5'TAC AGC	0.18	0.27
59	5'ACG TAA	0.18	0.27
119	5'CGA GGC	0.18	0.38
95	5'TGC GCC	0.20	0.42
54	5'TCT CAA	0.26	0.21
36	5'ACG CAA	0.27	0.18
38	5'GCA ACC	0.27	0.21
100	5'CCC GCT	0.27	0.3
64	5'ACA CTT	0.27	0.3

[a] A_f/A_0 is the ratio of the peak area at saturating daunomycin concentrations (A_f) relative to the peak area in the absence of the drug (A_0). $C_{1/2}$ is the estimated daunomycin concentration required to yield $\theta = 0.5 = (A - A_f)/(A_0 - A_f)$, where A is the area at any drug concentration C. The position of cleavage within the sequences listed is between the central dinucleotide.

sites. The magnitude of the quantity A_f/A_0 differs from the mean value by at least one standard deviation for these sites. Seven of these 10 sites are located at the end of a triplet sequence 5'$\frac{A}{T}$CG or 5'$\frac{A}{T}$GC, where the notation $\frac{A}{T}$ means that either an A or T residue may occupy the position. We believe that these triplets are the preferred daunomycin binding sites within the *tyr T* DNA fragment. Triplets of exactly this type were predicted to be preferred sites in the theoretical studies of Chen et al. (1985). We previously interpreted lower resolution DNase I footprinting data to indicate that daunomycin preferentially recognized sites containing adjacent GC base pairs, flanked by an AT base pair (Chaires et al., 1987). Our

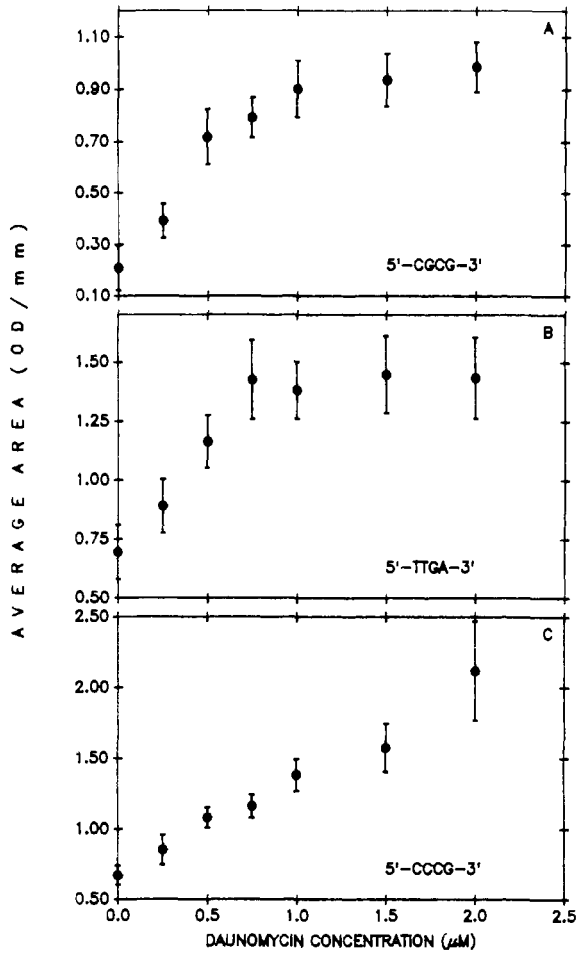

FIGURE 4: Selected examples of positions whose cleavage by DNase I is enhanced in the presence of daunomycin. These data are for the following positions within the sequence presented in Figure 6: (A) position 77; (B) position 85; (C) position 106.

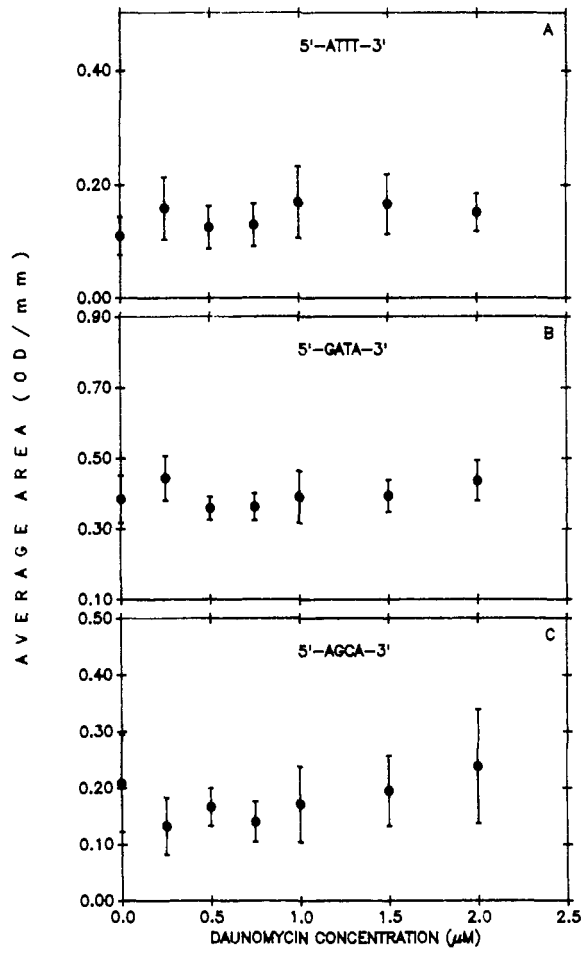

FIGURE 5: Example of positions whose cleavage by DNase I is unaffected by added daunomycin. These data are for the following positions within the sequence presented in Figure 6: (A) position 83; (B) position 87; (C) position 117.

current results are fully consistent with that general view, but the higher resolution of the footprinting titration method allows us to specify the preferred triplet sequence more exactly. In particular, an alternating purine/pyrimidine arrangement (CpG or GpC) appears to be the preferred arrangement of the adjacent GC base pairs within the triplet binding site. An AT base pair is consistently found at the 5'-end, but reversal of this base pair (TA versus AT) appears not to matter. In the remaining sites that do not contain this triplet motif (Table I), the dinucleotide sequence 5'CA or 5'CT may be found in two cases (positions 54 and 64), but these sites also are at the ends of the triplets 5'ACA or 5'TCT. The remaining site (position 67) is only one base pair away from the triplet 5'ACA (see Figure 6) and is also near the strongly protected site at position 70. These three cases suggest that the triplets 5'ACA or 5'TCT are also strongly protected daunomycin binding sites but that these are perhaps less preferred than sites containing contiguous GC base pairs.

We interpret the location of these strongly protected sites as follows. DNase I is a 31-kDa protein that covers approximately 10 bp on one side of the DNA double helix upon binding (Suck & Oefner, 1986). The crucial molecular interactions that stabilize the DNase I–DNA complex occur in the minor groove and involve the four base pairs to the 5'-side (with reference to the polarity of the strand that is cut) of the actual cleavage site. Ligand binding events that disrupt these minor groove interactions between DNase I and DNA thus may register as "protected" sites that are displaced in the 3'-direction relative to the actual ligand binding site. The ligand need not block the actual DNaseI cutting site in order to register a strong protection. This interpretation best accounts for the location of the sites strongly protected by daunomycin listed in Table I. Strong protection is observed at the 3'-end of the triplets $5'\frac{A}{T}CG$ or $5'\frac{A}{T}GC$ in seven of the 10 cases. Since daunomycin binds via the minor groove, protection at the observed sites most probably arises from strong daunomycin binding to the triplet sequence, resulting in blockage of the molecular interactions crucial for stable DNase I binding to the DNA and inhibition of strand cleavage at a distal site.

Further insight into the nature of preferred daunomycin binding sites results from consideration of all of the protected sites cataloged in Table S-I (supplementary material). We have resolved 40 protected sites, and in 20 of these cases, the protected site is at the end of a triplet sequence containing an AT base pair flanked by contiguous GC base pairs. These sites are marked by an asterisk in Table S-I. In 12 of the 20 cases, the two GC base pairs are in an alternating purine–pyrimidine arrangement. In contrast, we have identified 22 sites that are unaffected by added daunomycin (Table S-II). In only three cases are these sites at the end of the putative recognition triplet.

Data such as shown in Figure 2 may be transformed to show the fractional occupancy (θ) as a function of daunomycin concentration by the simple relation

$$\theta = (A_0 - A)/(A_0 - A_f)$$

where A_0 is the integrated peak area in the absence of drug,

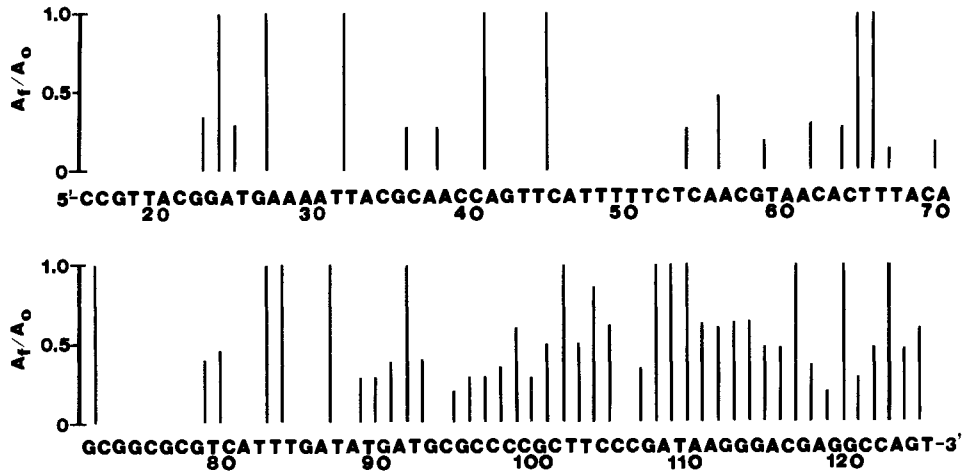

FIGURE 6: Summary of high-resolution footprinting results for the interaction of daunomycin with the *try T* DNA fragment. The sequence of the fragment is shown along with the numbering convention utilized to label individual bonds. The relative extent of protection for each resolved bond is indicated by the vertical bars, in terms of the quantity A_f/A_0, as defined in the text.

A_f the peak area at saturating drug concentrations, and A the peak area at any drug concentration C. If it is assumed that drug binding to individual sites is independent and that there are no interactions between sites, then the fractional occupancy is related to the binding constant K_i for each site by the relation

$$\theta = (K_iC)/(1 + K_iC) \quad (1)$$

where C is the *free* drug concentration. This relation makes it possible (if the simplifying assumptions are verified) to estimate the binding constant K_i at individual sites along the DNA lattice. Examples of sites that appear to follow this behavior are shown in the supplementary material (Figure S6). Analysis of the single-site isotherms for the 10 sites listed in Table I by eq 1 leads to estimates of K_i ranging from 0.4 to 1.8×10^7 M^{-1}. Since we know only the *total* daunomycin concentration in our experiments, not the *free*, these values represent an *underestimate* of the tree value K_i. We offer these estimates only to illustrate the quantitative potential of the footprinting titration experiment and to provide an order-of-magnitude estimate for the binding constants of these sites. Additional titration experiments with finer resolution over the daunomycin concentration range 0–0.25 μM are required to accurately determine the individual site binding constants.

A Second Class of Protected Sites. The footprinting titration experiment resolves a second class of protected sites whose behavior is illustrated in Figure 3. Initial additions of daunomycin show little effect on the band area of these sites, but at a threshold total drug concentration, the area is sharply reduced. The subtlety of the behavior of these sites was unobserved in previous daunomycin footprinting studies (Chaires et al., 1987; Skorobogaty, 1988a,b) and is revealed only in the footprinting titration procedure. Such behavior might result from binding to a class of sites with weaker affinity or from cooperative binding. Knowledge of the fractional occupancy of these sites as a function of *free* daunomycin concentration is required to distinguish these possibilities.

Enhanced Cleavage Sites. A third type of behavior, in which bond cleavage is enhanced, results from daunomycin binding (Figure 4). Table II lists the sites that show this behavior. We attribute the enhanced cleavage rate to alteration in the DNA structure induced by drug binding. An analysis of rate enhancements observed in footprinting experiments with netropsin and actinomycin D led to the suggestion that such effects arise from redistribution of enzyme

Table II: Sequences Showing Enhanced Cleavage by DNase I in the Presence of Daunomycin[a]

position	sequence	A_f/A_0	A_0
85	5'TTT GAT	2.1	0.7
48	5'CAT TTT	2.6	0.1
106	5'TCC GGA	3.2	0.7
77	5'GCG CGT	4.7	0.2

[a] A_0 is the peak area in the absence of daunomycin. A_f is the peak area at saturating concentrations of daunomycin. The position of cleavage within the sequences listed is between the central dinucleotide.

to unoccupied sites, following the law of mass action (Ward et al., 1988b; Dabrowiak & Goodisman, 1989). This explanation is unsatisfactory for our data. We observe a large number of sites that appear to be unaltered in any way over the range of daunomycin concentrations used in our studies (Figure 5, Table S-II). If mass action were to explain the enhanced cleavage phenomenon, all of these sites ought to uniformly show enhanced cleavage. A more likely explanation for the enhanced rate of cleavage at the limited number of sites that we observe is that the structure of these sites is perturbed to a form more susceptible to DNase I cleavage. Two types of sites that show enhanced cleavage are evident in Table II. Positions 85 and 48 are within oligo(dA)–oligo(dT) tracts. Oligo(dA)–oligo(dT) tracts adopt an unusual structure that is cut poorly by DNase I (Drew & Travers, 1984). We have shown directly that daunomycin binding renders poly(dA)–poly(dT) more susceptible to DNase I cleavage (Herrera & Chaires, 1989). The enhancements at positions 85 and 48 most probably result from an alteration of the unusual AT tract structure to a form more susceptible to DNase I digestion induced by daunomycin binding to nearby sites. Enhanced cleavage is observed at position 106 and 77, near putative triplet recognition sites. A plausible explanation for these enhancements is that they result from perturbed DNA structure in the immediate vicinity of an intercalation site. Crystallographic studies (Wang et al., 1987; Moore et al., 1989) show that base pairs away from the actual daunomycin intercalation site are unwound, which may result in greater susceptibility to DNase I cleavage. For reasons we do not understand, enhancements are not found near all preferred daunomycin binding sites we have been able to resolve.

Molecular Basis for Preferential Daunomycin Binding to $5'\frac{A}{T}GC$ *and* $5'\frac{A}{T}CG$. The results presented here establish that daunomycin preferentially binds to certain sequences along the DNA lattice in solution. Our analysis suggests that these

are the triplet sequences 5′$\frac{A}{T}$GC and 5′$\frac{A}{T}$CG. The molecular basis for preferential daunomycin binding to these sequences can be rationalized in light of recent crystallographic and theoretical studies. The structure of complexes of daunomycin bound to 5′d(CGTACG) (Wang et al., 1987) and to 5′d-(CGATCG) (Moore et al., 1989) are known to 1.2 Å and 1.5 Å, respectively. Theoretical studies have examined the sequence selectivity of daunomycin and several other anthracycline antibiotics in detail (Chen et al., 1985, 1986). Our results in solution are fully consistent with these theoretical and crystallographic studies. In the two crystal structures, daunomycin is intercalated between the CpG steps, with the daunosamine moiety extending down the minor groove to physically cover the AT base pair. Daunomycin is stabilized in the complex both by direct hydrogen bonds and by indirect hydrogen bonds mediated by water molecules. Certain molecular interactions are identified in both crystallographic studies. The O9 group of daunomycin forms two direct hydrogen bonds involving N2 and N3 of guanine within the central GC base pair of the complex. If adenine were substituted at this position, only a single hydrogen bond would be possible. A hydrogen bond is formed via a water molecule with the cytosine of the GC base pair at the end of the complex. In the major groove, O4 and O5 of the daunomycin chromophore and N7 of guanine from the terminal GC base pair are positioned to chelate either a sodium ion (Wang et al., 1987) or a water molecule (Moore et al., 1989). These interactions are probably key contributors to the preferred intercalation of daunomycin between the CpG step. We note that reversal of a GC base pair leaves the hydrogen bonding pattern accessible in the minor groove unchanged (Dickerson et al., 1987), thus daunomycin probably cannot discriminate between CpG or GpC steps, as indeed we observed in our footprinting results. The theoretical study of Chen et al. (1985) identified the daunomycin O9–guanine interaction as a key determinant in the preferential affinity of daunomycin toward the triplet 5′TCG, in agreement with what is observed in the crystal studies. The reason for the preference for an AT base pair at the 5′-end of the triplet is more subtle. Theoretical studies show that placement of a GC pair in that position results in repulsive interactions between the daunosamine and N2 of guanine (Chen et al., 1985). Observed molecular interactions involving the daunosamine with the 5′AT base pair differ in the two crystallographic studies, and it is not clear from these studies whether or not specific hydrogen bonds might contribute to sequence preference at this position.

Comparison with Other Daunomycin Footprinting Studies. The more refined results reported here are consistent with our previous footprinting efforts (Chaires et al., 1987). Another study of daunomycin sequence preference that used both DNase I footprinting and a RNA polymerase transcription inhibition assay concluded that daunomycin preferentially bound to the dinucleotide 5′CA (Skorobogaty et al., 1988a,b). The difference between this point of view and our proposed triplet specificity requires reconciliation. We first note that footprinting data are intrinsically incapable of establishing site sizes, because of the lack of *absolute* sequence specificity for most antibiotic–DNA interactions. Interpretation of footprinting data therefore usually requires an assumption about the site size. We assume a three bp site size, and therefore look for preferred triplet sequences, for several reasons. First, equilibrium binding studies have rigorously established that daunomycin binds to a three bp site [reviewed in Chaires (1990a)]. Single-crystal studies show that daunomycin physically occludes three bp upon complexation with an oligonucleotide, and that molecular interactions between the drug and DNA occur at all three base pairs (Wang et al., 1987; Moore et al., 1989). Finally, the theoretical studies of Chen et al. (1985) suggested that a triplet sequence was required to account for the specificity of daunomycin binding. If we look at the data of Skorobogaty et al. (1988a,b) in terms of a triplet recognition sequence, we find that in three of the seven protected sites they observe in a 180 bp restriction fragment from plasmid pSP65, the triplet 5′$\frac{A}{T}$GC may be found. In the remaining sites, the triplet 5′ACA may be found. Conversely, if we reexamine our previous footprinting data (Chaires et al., 1987), we find the dinucleotide 5′CA (or the equivalent 5′TG) 14 times in the 160 bp *try T* restriction fragment. In only six cases is the dinucleotide located within regions protected by daunomycin. In four of these six cases, the 5′CA sequence is within the triplet sequences 5′GCA, and in the remaining two case, it is part of the sequence 5′ACA. The eight 5′CA sequences that are not protected are not within triplet sequences of either of these two types. The data of Skorobogaty et al. (1988a,b) can be reconciled with our results as follows. If a triplet recognition site is assumed, preferred sites are identified as 5′$\frac{A}{T}$CG, 5′$\frac{A}{T}$GC, or 5′$\frac{A}{T}$CA. In our hands, the first two are the most preferred, but the latter is also a preferential daunomycin binding site. We note that the triplet 5′ACA or 5′TCA occurs in the strongly protected sites identified here that do not contain the 5′$\frac{A}{T}$CG motif (Table I). Considering the molecular basis of daunomycin sequence preference, this may mean that the 5′AT base pair and the central GC base pair are the predominant determinants for preferential binding. A very recent study (Trist & Phillips, 1989) that examined the specificity of Adriamycin, a closely related anthracycline antibiotic, has also suggested that the triplet 5′ACA is a preferred binding site. We believe that the apparent difference between our work and that of Skorobogaty et al. (1988a,b) arises primarily from differences in interpretation and that the primary experimental data obtained by the two groups are largely consistent.

Unique Aspects of the Daunomycin–DNA Interaction. Daunomycin is thus far unique among intercalators in its apparent recognition of a triplet sequence (Chen et al., 1985). The mixed-base composition of the triplet is a unique feature of the preferred daunomycin binding site. Daunomycin binding to its preferred site is stabilized by a combination of intercalation and minor groove interactions. Hydrogen bonding appears to play a key role in the sequence preference of daunomycin binding. This is in contrast to the groove binding antibiotics (netropsin, distamycin, Hoechst 2238), whose preferential binding to runs of AT base pairs is thought to arise primarily from the recognition of minor groove geometry (Dickerson et al., 1987). While hydrogen bonds certainly stabilize the complexes of these compounds with DNA, they do not appear to be the prime determinants of the sequence specificity (Dickerson et al., 1987). It is of interest that daunomycin binds poorly, if at all, to the sequences favored by these groove binding antibiotics.

Actinomycin, another complex intercalator, shows much more pronounced sequence specificity in footprinting experiments (van Dyke et al., 1982; Lane et al., 1983; Fox & Waring, 1984) and appears to bind selectively to the dinucleotide 5′GpC. However, spectroscopic and dialysis binding experiments utilizing natural DNA samples of varying GC content show that the apparent GC specificity of daunomycin is actually greater than that of actinomycin, based on the dependency of the overall equilibrium binding constant on

DNA base composition (Chaires, 1990b). That the daunomycin footprints are not as dramatic as those of actinomycin is therefore somewhat puzzling, and most probably arises from the pronounced differences in the binding kinetics between the two compounds.

Conclusions. High-resolution footprinting titration data indicate that daunomycin preferentially interacts with the triplet sequences 5′$\overset{A}{T}$CG and 5′$\overset{A}{T}$GC in solution. These results are in accord with two recent crystallographic studies, in which daunomycin is observed bound to the triplets 5′ACG (Wang et al., 1987) and 5′TCG (Moore et al., 1989). The theoretical studies of Chen et al. (1985) first predicted preferential binding of daunomycin to triplet sequences, with the sequences 5′ACG and 5′TCG being the most energetically favored of those studied. Solution, crystallographic, and theoretical studies have thus converged to provide a consistent and coherent view of the sequence preference of daunomycin. We caution, however, that the daunomycin sequence preference is not absolute and that the drug can and does bind to other triplets such as 5′$\overset{A}{T}$CA. The sequence preference of daunomycin reflects its unique mixed binding mode, in which the drug–DNA complex is stabilized by both intercalation and minor groove interactions. Hydrogen bonding interactions appear to be important contributors to the sequence preference, in possible contrast to the groove binding antibiotics like netropsin, for which minor groove geometry appears to be the primary determinant of their binding to preferred sequences. On the whole, the daunomycin–DNA interaction is now perhaps the best understood of the intercalation reactions. The fundamental understanding we now have concerning the binding of daunomycin to particular DNA sequences should be of value in the rational design of new anticancer compounds.

Supplementary Material Available

Six figures showing the densitometric scan of an autoradiogram, the linearity of the film response, the accuracy of the peak area determination, the total product area and band 45 area as a function of total daunomycin concentrations, the distribution A_f/A_0 values, and simple binding isotherms and tables of a catalog of protected sites and a catalog of sites unaffected by daunomycin (8 pages). Ordering information is given on any current masthead page.

Registry No. Daunomycin, 20830-81-3.

References

Arcamone, F. (1981) *Doxorubicin: Anticancer Antibiotics*, Academic Press, New York.

Brenowitz, M., Senear, D. F., Shea, M. A., & Ackers, G. (1986) *Methods Enzymol. 30*, 132–181.

Britt, M., Zunino, F., & Chaires, J. B. (1986) *Mol. Pharm. 29*, 74–80.

Chagas, C., & Pullman, B., Eds. (1987) *Molecular Mechanisms of Carcinogenic and Antitumor Activity*, Adenine Press, Inc., Schenectady, NY.

Chaires, J. B. (1983a) *Nucleic Acids Res. 11*, 8485–8494.

Chaires, J. B. (1983b) *Biochemistry 22*, 4204–4211.

Chaires, J. B. (1985a) *Biopolymers 24*, 403–419.

Chaires, J. B. (1985b) *Biochemistry 24*, 7479–7486.

Chaires, J. B. (1986) *J. Biol. Chem. 261*, 8899–8907.

Chaires, J. B. (1990a) *Biophys. Chem.* (in press).

Chaires, J. B. (1990b) in *Advances in DNA Sequence Specific Agents*, (Hurley, L. H., Ed.) Vol. 1, Jai Press (in press).

Chaires, J. B., Dattagupta, N., & Crothers, D. M. (1982a) *Biochemistry 21*, 3927–3932.

Chaires, J. B., Dattagupta, N., & Crothers, D. M. (1982b) *Biochemistry 21*, 3933–3940.

Chaires, J. B., Dattagupta, N., & Crothers, D. M. (1983) *Biochemistry 22*, 284–292.

Chaires, J. B., Dattagupta, N., & Crothers, D. M. (1985) *Biochemistry 24*, 260–267.

Chaires, J. B., Fox, K. R., Herrera, J. E. Britt, M., & Waring, M. J. (1987) *Biochemistry 26*, 8227–8236.

Chen, K.-X., Gresh, N., & Pullman, B. (1985) *J. Biomol. Struct. Dyn. 3*, 445–466.

Chen, K.-X., Gresh, N., & Pullman, B. (1986) *Mol. Pharm. 30*, 279–286.

Crooke, S. T., & Reich, S. D., Eds. (1980) *Anthracyclines: Current Status and New Developments*, Academic Press, New York.

Dabrowiak, J. C., & Goodisman, J. (1989) in *Chemistry & Physics of DNA-Ligand Interactions* (Kallenbach, N. R., Ed.) Adenine Press, Schenectady, NY.

Dickerson, R. E.; Kopka, M. L., & Pjura, P. E. (1987) in *DNA-Ligand Interactions: From Drugs to Proteins* (Gulschbauer, W., & Saenger, W., Ed.s) pp 45–62, Plenum Press, New York.

Drew, H. R., & Travers, A. A. (1984) *Cell 37*, 491–502.

Fox, K. R., & Waring, M. J. (1984) *Nucleic Acids Res. 12*, 9271–9285.

Fritzsche, H., & Berg, H. (1987) *Gaz. Chim. Ital. 117*, 331–352.

Fritzsche, H., Triebel, H., Chaires, J. B., Dattagupta, N., & Crothers, D. M. (1982) *Biochemistry 21*, 3940–3946.

Fritzsche, H., Wahnert, U., Chaires, J. B., Dattagupta, N., Schlessinger, F. B., & Crothers, D. M. (1987) *Biochemistry 26*, 8227–8236.

Gale, E. F., Cundliffe, E., Reynolds, P. E., Richmond, M. H., & Waring, M. J. (1981) *The Molecular Basis of Antibiotic Action*, 2nd ed., Wiley, London.

Herrera, J. E., & Chaires, J. B. (1989) *Biochemistry 28*, 1993–2000.

Lane, M. J., Dabrowiak, J. C., & Vournakis, J. W. (1983) *Proc. Natl. Acad. Sci. U.S.A. 80*, 3260–3264.

Low, C. M. L., Drew, H. R., & Waring, M. J. (1984a) *Nucleic Acids Res. 12*, 4865–4879.

Low, C. M. L., Olsen, R. K., & Waring, M. J. (1984b) *FEBS Lett. 176*, 414–420.

Moore, M. H., Junter, W. N., Langlois d'Estaintot, B., & Kennard, O. (1989) *J. Mol. Biol. 206*, 693–705.

Neidle, S., & Sanderson, M. R. (1983) in *Molecular Aspects of Anticancer Drug Action* (Neidle, S., & Waring, M. J., Eds.) pp 35–57, Verlag Chemie, Weinheim.

Remers, W. A., Ed. (1984) *Antineoplastic Agents*, John Wiley & Sons, Inc., New York.

Saenger, W. (1984) *Principles of Nucleic Acid Structure*, Springer-Verlag, New York.

Skorobogaty, A., White, R. J., Phillips, D. R., & Reiss, J. A. (1988a) *FEBS Lett. 227*, 103–106.

Skorobogaty, A., White, R. J., Phillips, D. R., & Reiss, J. A. (1988b) *Drug Des. Delivery 3*, 125–152.

Suck, D., & Oefner, C. (1986) *Nature 321*, 620–625.

Trist, H., & Phillips, D. R. (1989) *Nucleic Acids Res. 17*, 3673–3688.

Tullius, T. D. (1989) *Annu. Rev. Biophys. Biophys. Chem. 18*, 213–237.

Van Dyke, M. W., Hertzberg, R. P., & Dervan, P. B. (1982) *Proc. Natl. Acad. Sci. U.S.A. 79*, 5470–5474.

Wang, A. H.-J., Ughetto, G., Quigley, G. J., & Rich, A. (1987) *Biochemistry 26*, 1152–1163.
Ward, B., Rehfuss, R., & Dabrowiak, J. C. (1987) *J. Biomol. Struct. Dyn. 4*, 685–695.
Ward, B., Rehfuss, R., Goodisman, J., & Dabrowiak, J. C. (1988a) *Biochemistry 27*, 1198–1205.
Ward, B., Rehfuss, R., Goodisman, J., & Dabrowiak, J. C. (1988b) *Nucleic Acids Res. 16*, 1359–1369.

Mutagenesis by Site-Specific Arylamine Adducts in Plasmid DNA: Enhancing Replication of the Adducted Strand Alters Mutation Frequency†

Thomas M. Reid, Mei-Sie Lee, and Charles M. King*
Department of Chemical Carcinogenesis, Michigan Cancer Foundation, Detroit, Michigan 48201
Received January 29, 1990; Revised Manuscript Received March 13, 1990

ABSTRACT: Site specifically modified plasmids were used to determine the mutagenic effects of single arylamine adducts in bacterial cells. A synthetic heptadecamer bearing a single *N*-(guanin-8-yl)-2-aminofluorene (AF) or *N*-(guanin-8-yl)-2-(acetylamino)fluorene (AAF) adduct was used to introduce the adducts into a specific site in plasmid DNA that contained a 17-base single-stranded region complementary to the modified oligonucleotide. Following transformation of bacterial cells with the adduct-bearing DNA, putative mutants were detected by colony hybridization techniques that allowed unbiased detection of all mutations at or near the site of the adduct. The site-specific AF or AAF adducts were also placed into plasmid DNA that contained uracil residues on the strand opposite that bearing the lesions. The presence of uracil in one strand of the DNA decreases the ability of the bacterial replication system to use the uracil-containing strand, thereby favoring the use of the strand bearing the adducts. In a comparison of the results obtained with site specifically modified DNA, either with or without uracil, the presence of the uracil increased the mutation frequencies of the AF adduct by >7-fold to 2.9% and of the AAF adduct by >12-fold to 0.75%. The mutation frequency of the AF adduct was greatly reduced in a *uvrA*⁻ strain while no mutations occurred with the AAF adduct in this strain. The sequence changes resulting from these treatments were dependent on adduct structure and the presence or absence of uracil on the strand opposite the adducts. The AF adduct produced primarily single-base deletions in the absence of uracil but only base substitutions in the uracil-containing constructs. The AAF adduct produced mutations only in the uracil-containing DNA, which included both frame shifts and base substitutions. Mutations produced by both adducts were SOS dependent.

The formation of carcinogen–DNA adducts has been implicated in mutagenesis and carcinogenesis (Singer & Grunberger, 1983). Therefore, an understanding of the molecular mechanisms involved in the formation of mutations is important in determining how chemical carcinogens are involved in tumor formation. Most chemical mutagens produce reactive intermediates that damage DNA at multiple sites and may form more than one type of lesion (Singer & Grunberger, 1983). In addition, the local sequence of the DNA affects the degree to which a given base will react with a chemical as well as the mutational specificity at that site (Miller, 1983; Fuchs, 1984; Warpehoski & Hurley, 1988). The recent use of well-defined site-specific lesions in viral and plasmid genomes has allowed much greater control over both the identity of the adduct and the sequence context in which it resides (Basu & Essigmann, 1988). The mutagenic specificity of the two major adducts produced by aminofluorene derivatives, i.e., the AF[1] and AAF adducts of guanine, has been studied in a number of systems including those using site-specific constructs.

The mutagenic potential of these adducts is thought to be due in part to the distortion that each adduct causes in DNA. The acetylated AAF adduct can induce a conformational change in the DNA molecule by causing the modified guanine to rotate about the glycosidic bond into a syn conformation and insert the AAF moiety bound to guanine into the base-pairing region of the helix (Fuchs & Daune, 1972; Fuchs et al., 1976; Grunberger & Weinstein, 1978). A comparison of mutagenesis studies using aminofluorene derivatives shows that the AAF adduct appears to be primarily a frame-shift mutagen (Fuchs et al., 1981; Koffel-Schwartz et al., 1984). However, one study showed that a site-specific AAF adduct in a plasmid vector gave rise primarily to base-substitution mutations (Moriya et al., 1988), while in another sequence context a single AAF adduct produced only frame shifts (Burnouf et al., 1989). Furthermore, it has been shown that the presence of an AAF adduct in one strand of a double-stranded molecule can cause the loss of that strand such that only the unadducted strand will be used as a template for DNA replication (Koffel-Schwartz et al., 1987). Conformational studies of the nonacetylated AF adduct have shown that it prefers the normal

† This report from the A. Alfred Taubman Facility for Environmental Carcinogenesis Research was supported by NIH Grant CA45639 and an institutional grant from the United Foundation of Detroit.
* To whom correspondence should be addressed.

[1] Abbreviations: AF, *N*-(guanin-8-yl)-2-aminofluorene; AAF, *N*-(guanin-8-yl)-2-(acetylamino)fluorene; *N*-AcO-TFAAF, *N*-acetoxy-*N*-(trifluoroacetyl)-2-aminofluorene; *N*-AcO-AAF, *N*-acetoxy-*N*-acetyl-2-aminofluorene; AIX medium, LB agar containing 100 μg/mL ampicillin, 70 μg/mL IPTG, and 80 μg/mL X-Gal; bp, base pair; gapped heteroduplex, double-stranded plasmid DNA containing a 17-base gap in the minus strand; HPLC, high-performance liquid chromatography; SDS, sodium dodecyl sulfate, SSC, 150 mM sodium chloride and 15 mM sodium citrate (pH 7.0); TLC, thin-layer chromatography.

0006-2960/90/0429-6153$02.50/0